https://doi.org/10.3311/PPee.20287



**Periodica Polytechnica Electrical Engineering and Computer Science**, 66(3), pp. 227–235, 2022

# Modelling and Attitude Control of an Agile Fixed Wing UAV based on Nonlinear Dynamic Inversion

Stephen Kimathi[1*], Béla Lantos[1]

[1] Department of Control Engineering and Information Technology, Faculty of Electrical Engineering and Informatics, Budapest University of Technology and Economics, Magyar tudósok krt. 2., H-1117 Budapest, Hungary
[*] Corresponding author, e-mail: kimathi@iit.bme.hu

Received: 07 April 2022, Accepted: 10 May 2022, Published online: 31 May 2022

**Abstract**

An estimation model is key in the design and development of an unmanned aerial vehicle's control system. This work presents a complete methodology for modelling the dynamics of a fixed-wing UAV for aerobatic maneuvers. The UAV dynamic non-linear model considered uses total variables instead of a nominal values and perturbation values about certain trimmed conditions for conventional flight envelopes. Such modelling allows the expansion of the flight envelope of an unmanned aerial vehicle to cover the full range of the angle of attack. The quaternion formulation is used since it eliminates the nonlinearity of the aerodynamics due to Euler angles for high angle of attacks. The objective is to have a complete and accurate representation of a highly dynamic fixed wing UAV capable of making aerobatic maneuvers without encountering singularities. A set of controllers are then designed for the inner and outer loops for attitude control using nonlinear dynamic inversion in cascade with a PI controller. Simulations carried out show robust tracking of reference attitude angles.

**Keywords**

maneuvering aircraft, dynamic model, nonlinear dynamic inversion, fixed wing UAV, attitude

## 1 Introduction

An Unmanned Aerial Vehicle (UAV) is a powered vehicle that uses aerodynamic forces to provide lift and can fly autonomously or be piloted remotely. The design and configuration of a UAV can vary according to its specifications and applications. Even though UAVs can be built for any size, most designers tend to keep them small hence better energy efficiency and a low cost. UAVs can be categorized in terms of their mechanical architecture into three groups that is fixed wing, rotary wings and hybrid UAVs which combine the properties of both fixed wing and rotary wing UAVs.

The methodological modelling of a conventional aircraft has been provided in different literature. In [1], the equations of motion of a rigid aircraft are derived using the procedure attributed to Byran, whose basis is largely used. The aim was to realize the Newton's second law of motion for the six degrees of freedom. A linearization of the equations is done with the assumption of a steady flight and specific trim conditions. This method is similar to the one presented in [2] for small UAVs albeit using a different methodology.

The complete set of equations, reduced order models, separation into the longitudinal and lateral directional dynamics and the simplifications thereof are given in [1, 2] and expressed in first order form hence can be rearranged into the state vector form. If linearization is not carried out, there would be cross coupling; motion of the lateral dynamics would induce motion in the longitudinal dynamics and vice versa. A common challenge that the above method encounters with respect to representation of the attitude of an aircraft is the gimbal lock. This effect arises due to the angular velocities transformation from one axes to another using the 3-2-1 Euler angles [3]. The integration of the ensuing variables become indeterminate due to a singularity for values of $\theta = \pm 90°$.

A common way to avoid the singularity is to use a single rotation about an eigen axis/Euler axis to describe the orientation of a non-inertial frame relative to an inertial frame through a change of variables. This method is attributed to the Euler-Rodrigues quaternion formulation where the parameters in the Euler axis description

**Cite this article as:** Kimathi, S., Lantos, B. "Modelling and Attitude Control of an Agile Fixed Wing UAV based on Nonlinear Dynamic Inversion", Periodica Polytechnica Electrical Engineering and Computer Science, 66(3), pp. 227–235, 2022. https://doi.org/10.3311/PPee.20287

of orientation were used to define four parameters. These four parameters uniquely described an orientation having only three degrees of freedom [3].

This formulation is free from singularities in critical flying situations however, the interpretation of a quaternion is less intuitive than the Euler angles. Using this formulation and the Newton's approach, the translational and rotational states of any rigid body can be completely defined for a full flight envelope. For a highly dynamic flight, the nonlinear behavior would be difficult to capture using the conventional approach. This is the case in some particular maneuvers such as perching, aggressive turns and waypoint transitions. However, considerable research has been carried out in this area for a highly dynamic combat aircraft [4, 5] but the results cannot be applied to small fixed-wing UAVs due to their small size, low thrust to weight ratios, high aspect ratios and small control surfaces.

This paper is organized as follows; Section 2 describes the dynamics and the conventional model while Section 3 introduces the more general quaternion formulation. Section 4 discusses the forces and moments equations acting on an aircraft. Section 5 discusses the controller design based on nonlinear dynamic inversion in cascade with a PI controller. Physical properties of a UAV model are given in Section 6 and in Section 7, results and discussions of the simulations done are given.

## 2 Conventional model

The motion of an aircraft is described in terms of forces, moments, linear and angular velocities, and attitude resolved into components with respect to a chosen reference axis system. Central to this framework is the derivation of a mathematical model commonly referred to as the equations of motion. These are a set of equations describing the generalized six degrees of freedom, 6-DoF motion of a rigid vehicle in the body fixed frame [1, 6] and are given in Eq. (1) and Eq. (2).

$$\begin{aligned} m\left(\dot{U} - rV + qW\right) &= X \\ m\left(\dot{V} - pW + rU\right) &= Y \\ m\left(\dot{W} - qU + pV\right) &= Z \end{aligned} \tag{1}$$

$$\begin{aligned} I_x\dot{p} - \left(I_y - I_x\right)qr - I_{xx}\left(pq + \dot{r}\right) &= L \\ I_y\dot{q} + \left(I_x - I_z\right)pr + I_{xz}\left(p^2 - r^2\right) &= M \\ I_z\dot{r} - \left(I_x - I_y\right)pq + I_{xz}\left(qr - \dot{p}\right) &= N \end{aligned} \tag{2}$$

Equation (1) represents the forces equations which describe the motion of the center of gravity, and Eq. (2) is the moment equations with the variables on the right describing the rolling, pitching, and yawing motions respectively. The resulting forces and torques in CoG of the body frame are $F_B = (X, Y, Z)^T$ and $M_B = (L, M, N)^T$, respectively. The other variables have their meanings as provided for in literature [1].

These equations of motion were derived for an axis system fixed to the aircraft. However, the position and attitude of an aircraft is usually described relative to an inertial frame usually the earth fixed frame of reference. The orientation of these two coordinate systems relative to each other are provided using Euler angles transformations.

Let the inertial coordinate system be represented by $(x, y, z)$ and the body fixed axis by $(x_b, y_b, z_b)$. The Euler angle rotation sequence $\varphi_z \rightarrow \varphi_y \rightarrow \varphi_x$ with the associated angles $\psi, \theta, \phi$, respectively is the commonly used in the aeronautical community. The coordinate orientation transformation from the body fixed system to the inertial frame is described using the matrix $\boldsymbol{R}_B^I$ as in Eq. (3).

$$\boldsymbol{R}_B^I = \begin{bmatrix} C_\theta C_\psi & S_\phi S_\theta C_\psi - C_\phi S_\psi & C_\phi S_\theta C_\psi + S_\phi S_\psi \\ C_\theta S_\psi & S_\phi S_\theta S_\psi + C_\phi C_\psi & C_\phi S_\theta S_\psi - S_\phi C_\psi \\ -S_\theta & S_\phi C_\theta & C_\phi C_\theta \end{bmatrix} \tag{3}$$

The angular velocities $p, q, r$ in fixed body axes can also be related to the attitude rates $\dot{\phi}, \dot{\theta}, \dot{\psi}$ with respect to inertial frame [1]. In matrix form, it is expressed as

$$\begin{bmatrix} p \\ q \\ r \end{bmatrix} = \begin{bmatrix} 1 & 0 & -S_\theta \\ 0 & C_\phi & S_\phi C_\theta \\ 0 & -S_\phi & C_\phi C_\theta \end{bmatrix} \begin{bmatrix} \dot{\phi} \\ \dot{\theta} \\ \dot{\psi} \end{bmatrix},$$

or alternatively as in Eq. (4) after inversion.

$$\begin{bmatrix} \dot{\phi} \\ \dot{\theta} \\ \dot{\psi} \end{bmatrix} = \begin{bmatrix} 1 & S_\phi S_\theta / C_\theta & C_\phi S_\theta / C_\theta \\ 0 & C_\phi & -S_\phi \\ 0 & S_\phi / C_\theta & C_\phi / C_\theta \end{bmatrix} \begin{bmatrix} p \\ q \\ r \end{bmatrix} \tag{4}$$

Equation (4) provides the kinematic transformation in terms of Euler angles which allows us to represent and update the orientation of an aircraft with time. Notice that the 1st and the 3rd rows create a singularity when $\theta = \pm 90°$ [1]. This is called the gimbal lock. The four quantities go to infinity and the Euler angle integration becomes indeterminate. Sometimes, approximate models are used.

Often, the deterioration in the fidelity of the response resulting from the use of approximate models may be insignificant. The limit of the approximation is determined

by the ability of mathematics to describe the physical phenomena involved, or by the acceptable complexity of the description. In many fields of engineering, simplicity is a most desirable virtue.

The derivation of UAV dynamics incorporating Euler angles is classical and easy to implement. However, when more arduous designs and dynamics are to be considered, Euler angles encounter difficulties in the form of singularities and gimbal locks.

## 3 Quaternion formulation

Quaternions were proposed by Hamilton in the nineteenth century as a three-dimensional version of complex numbers. They are also known as 'hyper complex' numbers since they can be represented as one real and three imaginary numbers as $q \triangleq q_s + q_1\hat{i} + q_2\hat{j} + q_3\hat{k}$ where $\hat{i},\hat{j},\hat{k} \in I$, such that $\hat{i}^2 = \hat{j}^2 = \hat{k}^2 = \hat{i}\ \hat{j}\ \hat{k} = -1$ and $q_s, q_1, q_2, q_3 \in R$ [7].

In another assumption, the quaternion $q = (s, \boldsymbol{w})$ is a pair of a scalar $s = q_0$ and a vector $\boldsymbol{w} = (q_1, q_2, q_3)$. The conjugate of the quaternion is $\tilde{q} = (s, -\boldsymbol{w})$. The product of two quaternions is defined by

$$q_1 \otimes q_2 = (s_1 s_2 - w_1^T w_2, w_1 \times w_2 + s_1 w_2 + s_2 w_1) .$$

For application, the subset of unit norm quaternions plays an important role satisfying $||q|| = s^2 + \boldsymbol{w}^2 = 1$. It is well known that a general rotation $R$ around a unit axis $t$ by an angle $\varphi$ can be expressed by the Rodrigues formula

$$\boldsymbol{R} = I + (1 - C_\varphi)\left[t\times\right]^2 + S_\varphi\left[t\times\right],$$

where $C_\varphi = \cos(\varphi)$ and $S_\varphi = \sin(\varphi)$ are used. The orientation of the body frame to the inertia frame can be described by a unit norm quaternion according to

$$\boldsymbol{R}_B^I = I + 2s\left[w\times\right] + 2\left[w\times\right]\left[w\times\right],$$

where $s = C_{\varphi/2}$ and $w = S_{\varphi/2}t$. The formula can easily be converted to a form using only $q_0$, $q_1$, $q_2$, $q_3$ and the property $q_0^2 = 1 - (q_1^2 + q_2^2 + q_3^2)$:

$$\boldsymbol{R}_B^I = \begin{bmatrix} q_0^2 + q_1^2 - q_3^2 - q_2^2 & 2(q_1q_2 - q_0q_3) & 2(q_1q_3 + q_0q_2) \\ 2(q_1q_2 + q_0q_3) & q_0^2 + q_2^2 - q_3^2 - q_1^2 & 2(q_2q_3 - q_0q_1) \\ 2(q_1q_3 - q_0q_2) & 2(q_2q_3 + q_0q_1) & q_0^2 + q_3^2 - q_2^2 - q_1^2 \end{bmatrix}$$

Unit norm quaternions can be extensively used to represent dynamics, velocity and orientation of rigid bodies since they do not suffer the limitations associated with Euler angles in critical flight situations. Therefore, quaternions can play an integral part in tracking the orientation of a vehicle, thereafter construct the direction cosine matrix (DCM) and/or the Euler angles from the quaternions [7]. This is what makes them desirable for flight-modelling.

The compact equations of motion for a UAV describing the dynamics and orientation can be written as

$$\dot{V}_B^{cg} = \frac{1}{m}F_B - \omega_B \times V_B^{cg}, \tag{5}$$

$$\dot{\omega}_B = I_B^{-1}\left[M_B - \omega_B \times \left(I_B\omega_B\right)\right], \tag{6}$$

$$\dot{P}_I = R_B^I V_B^{cg}, \tag{7}$$

$$\dot{q} = \frac{1}{2}q \otimes \omega_B . \tag{8}$$

Using quaternions, the model of a complete flight envelope of a UAV will be captured to encompass ±90° range in the sideslip angle and angle of attack. Due to the advantages stated, a quaternion, $q$ is used to represent attitude. The translational velocity $V_B^{cg} = \left[u, v, w\right]^T$, angular velocity $\omega_B = [p, q, r]^T$, inertia matrix $I_B$, forces $F_B$ and moments $M_B$ acting on an aircraft are resolved in the body frame while the position vector $\boldsymbol{P}_I = [x, y, z]^T$ is resolved in the inertial frame. $\boldsymbol{R}_B^I$ is the quaternion rotation matrix transformation from the body frame to the inertial frame. Equation (8) which is a quaternion product, is fully represented as in Eq. (9).

$$\dot{q} = \frac{1}{2}q \otimes \omega_B = \frac{1}{2}\begin{bmatrix} -q_1p - q_2q - q_3r \\ q_0p + q_2r - q_3q \\ q_0q + q_3p - q_1r \\ q_0r + q_1q - q_2p \end{bmatrix}, \tag{9}$$

which provides the kinematic transformation equations in terms of a quaternion of finite rotation [7].

## 4 Forces and torques

The total forces and moments acting on an aircraft due to aerodynamics, propulsion and gravitational effects are given in Eq. (10).

$$\begin{aligned} F_B &= F_B^{grav} + F_B^{prop} + F_B^{aero} \\ M_B &= M_B^{prop} + M_B^{aero} \end{aligned} \tag{10}$$

The gravitational force which is usually expressed in an inertial frame must be transformed to the body frame since the aerodynamic and propulsion forces are expressed in the body frame. The aerodynamics forces and moments include the contribution due to the aerodynamic control deflections that is, the elevator, aileron and rudder. Roll control stick, pitch control stick and rudder pedal displacements will be denoted by $\delta_a$, $\delta_e$ and $\delta_r$, respectively for a standard aircraft configuration.

For the v-tail configuration ruddervators are used. They are two movable surfaces on the V-tail empennage. The differential displacement of ruddervators achieves the same effect as the rudder and the simultaneous displacement same effect as an elevator. In the flying wing-configuration, the differential displacement of elevons has same effect as ailerons and simultaneous displacement the effect of an elevator. Fig. 1 shows the two configurations.

### 4.1 Propulsion

For completeness, propeller forces and moments are expressed as in Eq. (11).

$$\begin{aligned} F_B^{Prop} &= \left[T, F_{y,p}, F_{z,p}\right] \\ M_B^{Prop} &= \left[Q, M_{y,p}, M_{z,p}\right] \end{aligned} \tag{11}$$

$T$ is the force, $Q$ is the torque, $F_{y,p}$ is the side force, $F_{z,p}$ is the normal force, $M_{y,p}$ is the pitching moment and $M_{z,p}$ is the yawing moment. Due to the rotation of a propeller, a slipstream is created. The slipstream contributes more airflow over the aircraft surfaces. A rotating propeller of a maneuverable aircraft propulsion system induces flow in three directions: axial, radial and swirl. The radial and swirl components are normally neglected [6].

### 4.2 Aerodynamics

The forces and moments describing the longitudinal dynamics are influenced by the pitch rate, $q$ and elevator deflection, $\delta_e$ [6]. The contribution of aerodynamic forces and moments from other different components/segments are neglected. In the lateral dynamics, the forces and moments are influenced by the sideslip angle $\beta$, roll rate $p$, yaw rate $r$ and control deflections $\delta_a$ and $\delta_r$. Using Taylor series approximations, the resultant forces and moments are given by Eq. (12) and Eq. (13).

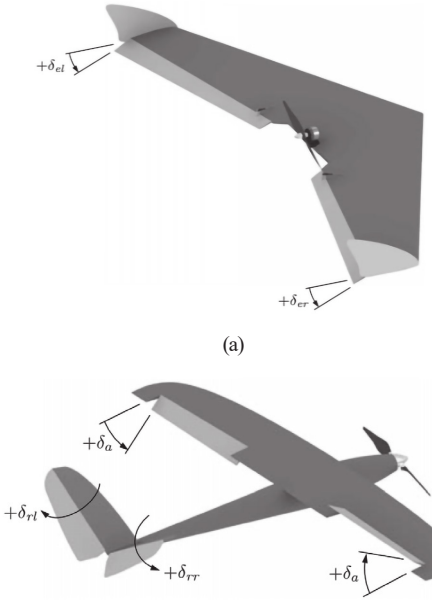


**Fig. 1** (a) Elevons and (b) Ruddervators in a UAV [2]

$$\begin{aligned} F_x^{aero} &= \frac{1}{2}\rho V_a^2 bc\left[C_{Lq}\frac{c}{2V_a}q + C_{L\delta e}\delta e\right] \\ F_y^{aero} &= \frac{1}{2}\rho V_a^2 bc\begin{bmatrix} C_{y\beta}\beta + C_{yp}\dfrac{b}{2V_a}p + C_{yr}\dfrac{b}{2V_a}r \\ +C_{y\delta a}\delta a + C_{y\delta r}\delta r \end{bmatrix} \\ F_z^{aero} &= \frac{1}{2}\rho V_a^2 bc\left[C_{Dq}\frac{c}{2V_a}q + C_{D\delta e}\delta e\right] \end{aligned} \tag{12}$$

$$\begin{aligned} M_x^{aero} &= \frac{1}{2}V_a^2 b^2 c\begin{bmatrix} C_{l\beta}\beta + C_{lp}\dfrac{b}{2V_a}p + C_{lr}\dfrac{b}{2V_a}r \\ +C_{l\delta a}\delta a + C_{l\delta r}\delta r \end{bmatrix} \\ M_y^{aero} &= \frac{1}{2}\rho V_a^2 bc^2\left[C_{m\alpha}\alpha + C_{mq}\frac{c}{2V_a}q + C_{m\delta e}\delta e\right] \\ M_z^{aero} &= \frac{1}{2}\rho V_a^2 b^2 c\begin{bmatrix} C_{n\beta}\beta + C_{np}\dfrac{b}{2V_a}p + C_{nr}\dfrac{b}{2V_a}r \\ +C_{n\delta a}\delta a + C_{n\delta r}\delta r \end{bmatrix} \end{aligned} \tag{13}$$

The different equations and relations given in the preceding text are plugged into Eq. (5) and Eq. (6). The resulting Eq. (14) and Eq. (15) are the 6 DoF equations that can be used to describe the motion of a highly maneuverable fixed wing UAV.

$$\begin{bmatrix}\dot{u}\\ \dot{v}\\ \dot{w}\end{bmatrix} = \begin{bmatrix} rv - qw \\ pw - ru \\ qu - pv \end{bmatrix} + g\begin{bmatrix} 2(q_1q_3 + q_0q_2) \\ 2(q_2q_3 + q_0q_1) \\ q_0^2 + q_3^2 - q_1^2q_2^2 \end{bmatrix} + \frac{1}{m}(F_B^{aero} + F_B^{prop}) \tag{14}$$

$$\begin{bmatrix}\dot{p}\\ \dot{q}\\ \dot{r}\end{bmatrix} = I_B^{-1}\left(\begin{bmatrix} (I_y - I_z)qr + I_{xz}pq \\ (I_z - I_x)pr + I_{xz}(r^2 - p^2) \\ (I_x - I_y)pq + I_{xz}qr \end{bmatrix} + M_B^{aero} + M_B^{prop}\right) \tag{15}$$

These equations rewritten in compact form become

$$\begin{aligned} \dot{v}_B &= -\omega_B \times v_B + g\left(R_B^I\right)^T (0,0,1)^T + \frac{1}{m}\left(F_B^{aero} + F_B^{prop}\right) \\ \dot{\omega}_B &= I_B^{-1}\left(-\omega \times \left(I_B\omega\right) + M_B^{aero} + M_B^{prop}\right) \end{aligned}$$

The aircraft kinematics are described by Eq. (16) using quaternions which defines the vehicle position with respect to an inertial frame.

$$\begin{bmatrix} \dot{x}_E \\ \dot{y}_E \\ \dot{z}_E \end{bmatrix} = \begin{bmatrix} q_0^2+q_1^2-q_3^2-q_2^2 & 2(q_1q_2-q_0q_3) & 2(q_1q_3+q_0q_2) \\ 2(q_1q_2+q_0q_3) & q_0^2+q_2^2-q_3^2-q_1^2 & 2(q_2q_3-q_0q_1) \\ 2(q_1q_3-q_0q_2) & 2(q_2q_3+q_0q_1) & q_0^2+q_3^2-q_2^2-q_1^2 \end{bmatrix} \begin{bmatrix} u \\ v \\ w \end{bmatrix} \tag{16}$$

The orientation is calculated using Eq. (4), which represent the aircraft attitude using Euler angles. In case of singularities, the Euler angles are computed from quaternions using Eq. (17).

$$\begin{bmatrix} \phi \\ \theta \\ \psi \end{bmatrix} = \begin{bmatrix} \text{atan2}\,(2(q_0q_1+q_2q_3),\ q_0^2+q_3^2-q_1^2-q_2^2) \\ \text{asin}\,(2(q_0q_2-q_1q_3)) \\ \text{atan2}\,(2(q_0q_3+q_1q_2),\ q_0^2+q_1^2-q_2^2-q_3^2) \end{bmatrix} \tag{17}$$

## 5 Controller design

For a conventional fixed wing UAV the control segments are the ailerons, elevator and rudder deflections, defined as variables $\delta_a$, $\delta_e$ and $\delta_r$. The outputs are the roll, pitch, and yaw angles $(\phi, \theta, \psi)$ and angular velocity rates $(p, q, r)$, respectively. The control goal for a hierarchical control strategy is to control the inner loop through stabilizing the nonlinear dynamics.

The inner loop as shown in Fig. 2 are fast dynamics and correspond to the states $(p, q, r)$. That is, for any given reference attitude angles, the inner loop control will track the desired angular rates for the reference attitude angles. The outer loop consists of variables as shown in Fig. 2 which provide references and trajectories to be tracked by the nonlinear model of the aircraft. In order to achieve these objectives, a closed loop cascade control structure is adopted.

The inner control method using Nonlinear Dynamic Inversion (NLDI) stabilizes the dynamics and the outer reference tracking method is conjured using a proportional integral (PI) controller. Usually, the integral term in a PI controller reduces the steady state error, and the corrective action is proportional to the deviation from the target. The outer loop should provide continuous reference signals to the inner loop that is why PI controller is desirable. Moreover, a PI controller is simple to implement, highly sensitivity and effective even in the presence of nonlinearities.

### 5.1 Nonlinear Dynamic Inversion

Linear flight models capture the approximate motion of a vehicle under specific conditions. From these models, linear flight control systems are normally derived. However, due to the approximate motions, robustness and good performance cannot be guaranteed especially for an agile aircraft due to the nonlinearities and saturations that limit linear approximation. Therefore, linear analysis is not suited for these applications.

Nonlinear control methods remedy the limitations of linear control methods. One common candidate approach is nonlinear dynamic inversion, which involves transforming a nonlinear model into a full or partial model using differential-algebraic means. The fundamental principle of dynamic inversion is to obtain a nonlinear controller for a system using an inverse transformation using algebraic means to cancel a nonlinearity from the input to the output (input/output linearization). This is done by enforcing stable linear error dynamics. The advantages are that it leads to a simple design, no need of tedious gain scheduling, has an easy online implementation as it leads to a 'closed form solution' for a controller and it is guaranteed asymptotic stability for the error dynamics. The downside of this method is sensitive to modeling inaccuracies and unlike linear methods, this approach in most cases arrives at a model dependent controller.

Unfortunately, the approach may have two problems. Firstly, in case of underactuated systems besides the linearized subsystem, a nonlinear zero dynamics also arises that may be unstable. Secondly, also in case of fully actuated systems without zero dynamics, the aerodynamic

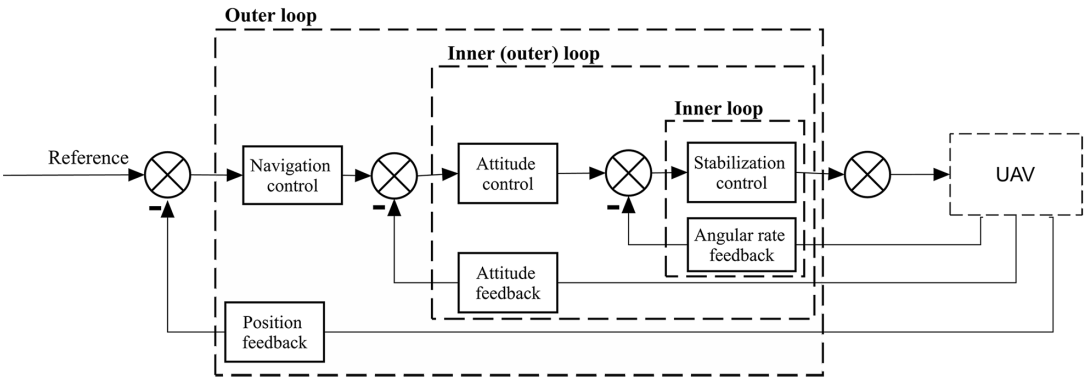


**Fig. 2** Cascade Inner and Outer Loop Control Architecture

forces and moments acting on an agile aircraft present complex non-linearities that are difficult to model accurately, and thus perfect cancellation due to dynamic inversion becomes arduous. Moreover, any unmodelled dynamics and parameter uncertainty contribute to reducing the robustness of a controller designed using NLDI.

Nonetheless, due to its simple design and asymptotic stability, NLDI can be very useful in aircraft controller design [8].

### 5.2 Input/output linearization of the orientation

The orientation subsystem is fully actuated and can be brought to the form

$$I_c\dot{\omega}_B + \omega_B \times (I_c\omega_B) = M_a + M_c\delta\,, \tag{18}$$

where the control signal is $\delta = (\delta a, \delta e, \delta r)^T$. The controller consists of a nonlinear and a linear part. The nonlinear controller can be chosen in the form

$$M_c\delta := I_c u + \omega_B \times (I_c\omega_B) - M_a\,. \tag{19}$$

Then the closed loop system will satisfy

$$I_c\dot{\omega}_B + \omega_B \times (I_c\omega_B) = M_a + \{I_c u + \omega_B \times (I_c\omega_B) - M_a\},$$
$$I_c\dot{\omega}_B = I_c u \Leftrightarrow \dot{\omega}_B = u,$$

which is a set of decoupled integrators. Hence, decoupled linear controllers can be chosen to satisfy

$$\dot{\omega}_B = u := \dot{\omega}_{B,ref} + PI$$
$$= \dot{\omega}_{B,ref} + k_P(\omega_{B,ref} - \omega_B) + k_I\int(\omega_{B,ref} - \omega_B)d\tau,$$

and with the error signal $e := (\omega_{B,\mathrm{ref}} - \omega_B)$ the resulting closed loop and its characteristic equation will be

$$\ddot{e} + k_P\dot{e} + k_I = 0 \Leftrightarrow s^2 + k_P s + k_I = 0. \tag{20}$$

Assuming $(1 + sT)^2$ with an appropriately chosen time constant $T$ the choice $k_p = 2/\mathrm{T}$, $k_I = 1/\mathrm{T}^2$ of the parameters should stabilize the system. With the low level linear controller $u := \dot{\omega}_{B,\mathrm{ref}} + PI$ the high level nonlinear controller to be realized is

$$\delta := M_c^{-1}\{I_c u + \omega_B \times (I_c\omega_B) - M_a\}. \tag{21}$$

Notice that for the realization, we need the aerodynamic model such that

$$M_a + M_c\delta = \frac{1}{2}\rho V^2 A\,\mathrm{diag}(b,\bar{c},b)(L,M,N)^T\,, \tag{22}$$

where $(L, M, N)$ are the dimension-free effects in the control torques reduced to the origin of the body frame that contain the control signal $\delta$ in linear form.

### 5.3 Cascaded PI controller

The inner (outer) loop of Fig. 2 was implemented using a PI controller cascaded with the non-linear dynamic inversion controller for the inner loop. This cascade architecture has been applied in [9, 10]. The aim of the cascade strategy is to provide continuous reference signals to the inner loop. These reference signals are the desired angular rates. The control law is expressed as

$$u = k_1 e + k_2\int_0^t e d\tau\,, \tag{23}$$

where $e_{\in(\phi,\theta,\psi)}$ is the error between the reference and current attitude angles, $k_{i\in 2}$ the PI controller gains and $u_{\in(p,q,r)}$ the desired angular rates. Although the attitude dynamics are almost decoupled, PI controllers are designed for each axis separately but with similar gains since the UAV is assumed to be symmetrical.

### 5.4 Velocity control

Velocity is normally controlled indirectly using the relation Eq. (24)

$$\dot{V}_a = \frac{F_{thrust}}{m} - \frac{F_{drag}}{m} - g\sin\gamma\,, \tag{24}$$

where $F_{thrust}$ is the thrust force, $F_{drag}$ is the drag, $g$ the gravitational pull and $\gamma$ the flight path angle. In this relation, thrust force can be used as the control variable for velocity. Consider,

$$\dot{V}_a = \frac{F_{thrust}}{m} - \frac{F_{drag}}{m} - g\sin\gamma =: g_0 + h_0 F_{thrust},$$
$$F_{thrust} = \left(\dot{V}_a - g_0 + K\right)/h_0, \tag{25}$$

where $K$ is the design parameter and it is chosen according to the velocity error given in Eq. (26) after appropriate substitutions.

$$\dot{V}_a = \dot{V}_{a,d} + K$$
$$e_{v_a} = V_{a,d} - V_a \Rightarrow \dot{e}_{v_a} = \dot{V}_{a,d} - \dot{V}_a \tag{26}$$

## 6 Aircraft parameters and geometric characteristics

The UAV used for simulations in this work is a Yak-54 reduced model [11]. The nominal values are, $C_{L_0} = 0.1470$, $C_{D_0} = 0.0528$, $C_{m_0} = -0.0008$, $C_{T_{x_0}} = 0.0515$, $M = 0.106$ and Oswald's efficiency factor was chosen as $k_o = 0.90$. The physical properties are given in Table 1.

Other aerodynamic properties, stability derivatives and parameters are listed in Table 2.

**Table 1** Aircraft properties

| Property | Value |
|---|---|
| $m$ | 12.755 kg |
| $I_x$ | 1.3059 kgm$^2$ |
| $I_y$ | 3.9208 kgm$^2$ |
| $I_z$ | 5.1597 kgm$^2$ |
| $I_{xz}$ | 0.0500 kgm$^2$ |
| $b$ | 2.4079 m |
| $c$ | 0.4420 m |
| Aspect ratio | 5.77 |

**Table 2** Stability and control derivatives

| Longitudinal derivatives (1/rad) | | Lateral derivatives (1/rad) | |
|---|---|---|---|
| $C_{D_u}$ | 0.0011 | $C_{y_\beta}$ | -0.3462 |
| $C_{D_\alpha}$ | -0.0863 | $C_{y_p}$ | 0.0073 |
| $C_{L_u}$ | 0.0017 | $C_{y_r}$ | 0.2372 |
| $C_{L_\alpha}$ | 4.5363 | $C_{l_\beta}$ | -0.0255 |
| $C_{L_{\dot{\alpha}}}$ | 1.9314 | $C_{l_p}$ | -0.3817 |
| $C_{L_q}$ | 5.1515 | $C_{l_r}$ | 0.0504 |
| $C_{m_u}$ | 0.0004 | $C_{n_\beta}$ | 0.0954 |
| $C_{m_\alpha}$ | -0.3701 | $C_{n_p}$ | -0.0156 |
| $C_{m_{\dot{\alpha}}}$ | -4.4705 | $C_{n_r}$ | -0.1161 |
| $C_{m_q}$ | -8.5026 | $C_{y_{\delta r}}$ | 0.1928 |
| $C_{L_{\delta e}}$ | 0.3762 | $C_{l_{\delta a}}$ | 0.3490 |
| $C_{m_{\delta e}}$ | -0.8778 | $C_{l_{\delta r}}$ | 0.0154 |
| $C_{D_q}$ | 0 | $C_{n_{\delta a}}$ | -0.0088 |
| $C_{D_{\delta e}}$ | 0 | $C_{n_{\delta r}}$ | -0.0996 |

## 7 Simulation tests

The proposed method was verified using simulations in Matlab Simulink. The dynamic model in Eq. (1) and Eq. (2) was implemented together with the kinematic model utilizing the quaternions Eq. (17). The design parameters were selected as $T = 50$ ms, $k_1 = 8$ and $k_2 = 16$.

### 7.1 Reference tracking of roll and yaw rates

The inner loop controller was tested first. Two signals were desired to be tracked simultaneously at the same simulation instance. Reference angular rates comprising 1 cycle of square wave signals with amplitude 0.5 *rad*/s and 0.25 *rad*/s were applied to the roll rate and yaw rate channels, respectively.

The results achieved from the inner loop are presented in Fig. 3. Both the rates were tracked well. This shows the robustness of nonlinear dynamic inversion in tracking the fast changing inner loop variables. The velocities, quaternions and the attitude angles are shown in Fig. 4 and Fig. 5, respectively.

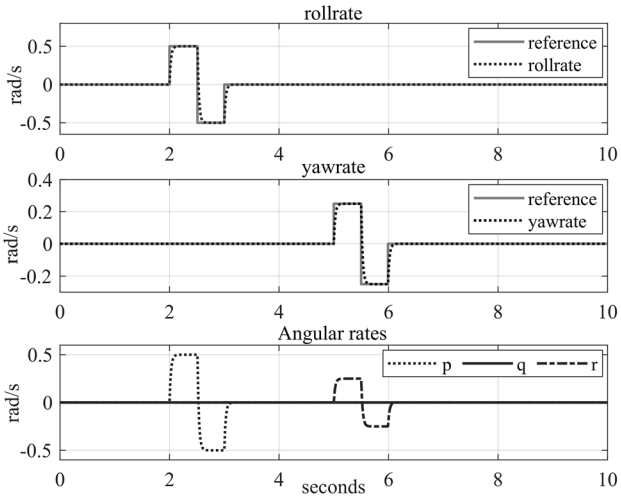


**Fig. 3** Roll and yaw rates tracking

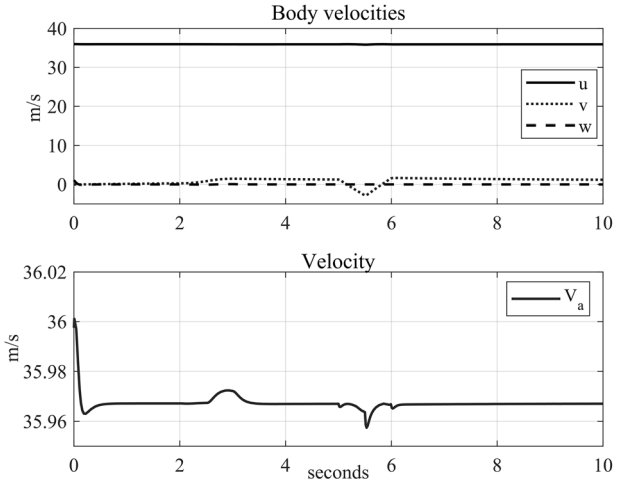


**Fig. 4** Velocities

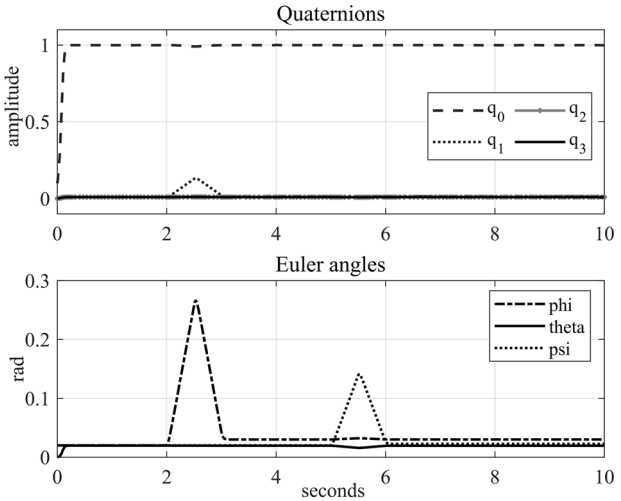


**Fig. 5** Quaternions and Euler angles

The total velocity decreased slightly from the steady state value by approximately 0.03 $ms^{-1}$. The quaternions in Eq. (9) were propagated using the concept given in [2].

Having established that the inner closed loop is stable and gives satisfactory results in tracking of reference angular rates, we embarked on attitude angle tracking via the outer loop. Arbitrary reference attitude angles with step changes of 0.53 *rad* and 0.27 *rad* for the roll angle and yaw angles, respectively were set. The output of the PI controller would provide the reference signals for the inner loop in a cascade architecture as in Fig. 2. Fig. 6 shows the roll angle and yaw angle tracking.

Good tracking performance is seen without any overshoots in both angles. The angular rates arising from this tracking are shown in Fig. 7. These provided the reference angular rates for the inner loop.

Tracking of these angular rates is shown in Fig. 8.

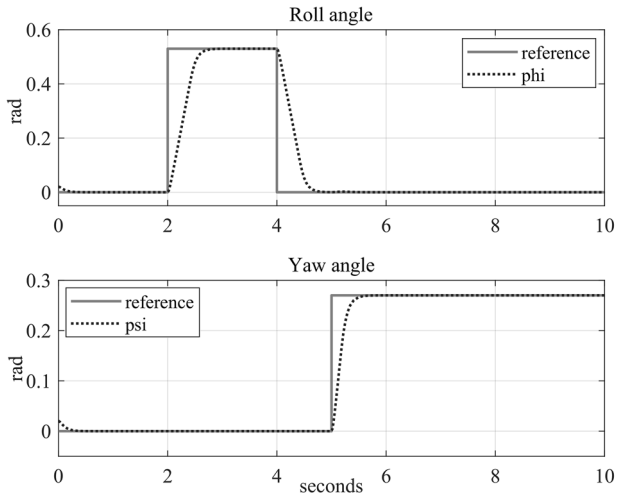


**Fig. 6** Roll and Yaw angles tracking

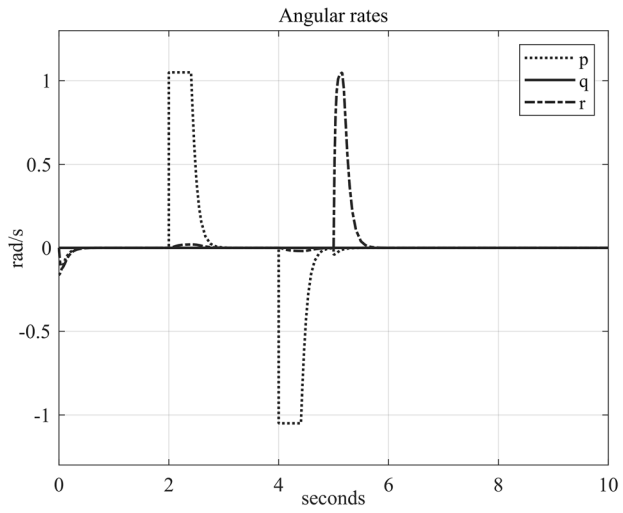


**Fig. 7** Desired angular rates

The quaternions and Euler angles during the simulation are as shown in Fig. 9. Fig. 10 shows the evolution of the body velocities and total velocity during the simulation.

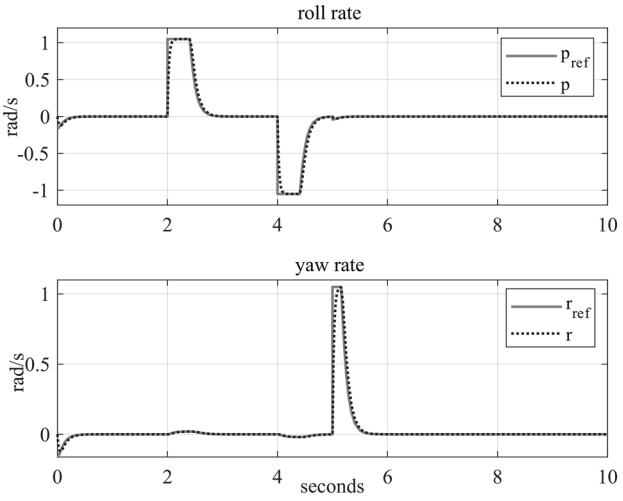


**Fig. 8** Reference angular rates tracking

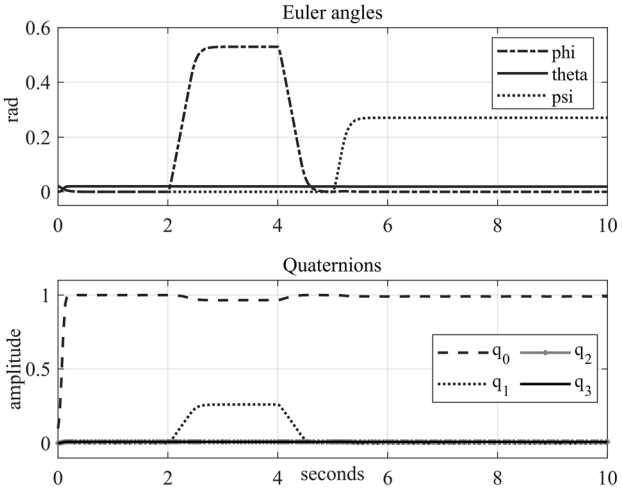


**Fig. 9** Euler angles and quaternions

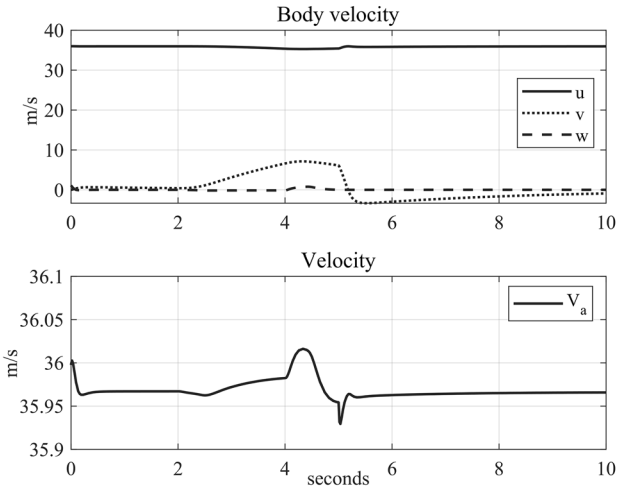


**Fig. 10** UAV velocity during simulation

## 8 Conclusions

A cascade control architecture has been presented for tracking of attitude angles in a fixed wing UAV. Based on the general flight dynamic equations, an inner loop controller was designed using nonlinear dynamic inversion to stabilize the inner loop fast evolving variables characterizing the angular body rates, and a PI controller for the outer loop to provide the inner loop with the desired reference body rates to achieve asymptotic tracking of the attitude angles. Numerical simulations carried out using the dynamic model of a Yak-54 reduced model show the effectiveness of the nonlinear dynamic inversion controller in a cascaded architecture with a PI controller in tracking reference attitude angles.

## References

[1] Cook, M. V. "Flight Dynamics Principles", Butterworth-Heinemann, 2007. ISBN: 978-0-7506-6927-6

[2] Beard, R. W., McLain, T. W. "Small Unmanned Aircraft", Princeton University Press, 2012. ISBN: 9781400840601 https://doi.org/10.1515/9781400840601

[3] Altmann, S. L. "Hamilton, Rodrigues and the Quaternion scandal", Mathematics Magazine, 62(5), pp. 291–308, 1989. https://doi.org/10.1080/0025570X.1989.11977459

[4] McCormick, B. W. "Aerodynamics, Aeronautics and Flight Mechanics", John Wiley and Sons, 1994. ISBN: 978-0-471-57506-1

[5] Stevens, B. L., Lewis, F. L., Johnson, E. N. "Aircraft Control and Simulation: Dynamics, Controls Design, and Autonomous Systems", Wiley-Blackwell, 2015. ISBN: 978-1-118-87098-3

[6] Waqas, K., Meyer, N. "Modeling Dynamics of Agile Fixed Wing UAVs for Real-Time Applications", In: 2016 International Conference on Unmanned Aircraft Systems (ICAUS), Arlington, VA, USA, 2016, pp. 1302–1312. ISBN:978-1-4673-9334-8 https://doi.org/10.1109/ICUAS.2016.7502599

[7] Phillips, W. F., Hailey, C. E., Gebert, G. A. "Review of Attitude Representations Used for Aircraft Kinematics", Journal of Aircraft, 38(4), pp. 718–737, 2001. https://doi.org/10.2514/2.2824

[8] Snell, S. A., Enns, D. F., Garrard, W. L. "Nonlinear Inversion Flight Control for a Supermaneuverable Aircraft", Journal of Guidance, Control and Dynamics, 15(4), pp. 976–984, 1992. https://doi.org/10.2514/3.20932

[9] Zhou, W., Yin, K., Wang, R., Wang, Y.-E. "Design of Attitude Control System for UAV Based on Feedback Linearization and Adaptive Control", Mathematical Problems in Engineering, 2014, 492680, 2014. https://doi.org/10.1155/2014/492680

[10] Poksawat, P., Wang, L., Mohamed, A. "Gain Scheduled Attitude Control of Fixed-Wing UAV With Automatic Controller Tuning", IEEE Transactions On Control Systems Technology, 26(4), pp. 1192–1203, 2017. https://doi.org/10.1109/TCST.2017.2709274

[11] Keshmiri, S., Leong, E., Jager, R., Hale, R. "Modeling and Simulation of the Yak-54 Scaled Unmanned Aerial Vehicle Using Parameter and System Identification", In: AIAA Atmospheric Flight Mechanics Conference and Exhibit, Honolulu, USA, 2008, pp. 1–15. eISBN: 978-1-60086-998-3 https://doi.org/10.2514/6.2008-6900